






Volume Regulation and Nonosmotic Volume of Individual Human Platelets Quantified by High-Speed Scanning Ion Conductance Microscopy

Konstantin Krutzke¹  Jan Seifert¹  Meinrad Gawaz²  Johannes Rheinlaender¹ 
Tilman E. Schäffer¹ 

¹Institute of Applied Physics, University of Tübingen, Tübingen, Germany

²Department of Internal Medicine III, Cardiology and Angiology, University of Tübingen, Tübingen, Germany

Address for correspondence Tilman E. Schäffer, PhD, Institute of Applied Physics, University of Tübingen, Auf der Morgenstelle 10, 72076 Tübingen, Germany
(e-mail: tilman.schaeffer@uni-tuebingen.de).

Thromb Haemost

Abstract

Background Platelets are anucleate cells that play an important role in wound closure following vessel injury. Maintaining a constant platelet volume is critical for platelet function. For example, water-induced swelling can promote procoagulant activity and initiate thrombosis. However, techniques for measuring changes in platelet volume such as light transmittance or impedance techniques have inherent limitations as they only allow qualitative measurements or do not work on the single-cell level.

Methods Here, we introduce high-speed scanning ion conductance microscopy (HS-SICM) as a new platform for studying volume regulation mechanisms of individual platelets. We optimized HS-SICM to quantitatively image the morphology of adherent platelets as a function of time at scanning speeds up to 7 seconds per frame and with 0.1 fL precision.

Results We demonstrate that HS-SICM can quantitatively measure the rapid swelling of individual platelets after a hypotonic shock and the following regulatory volume decrease (RVD). We found that the RVD of thrombin-, ADP-, and collagen-activated platelets was significantly reduced compared with nonactivated platelets. Applying the Boyle–van't Hoff relationship allowed us to extract the nonosmotic volume and volume fraction on a single-platelet level. Activation by thrombin or ADP, but not by collagen, resulted in a decrease of the nonosmotic volume, likely due to a release reaction, leaving the total volume unaffected.

Conclusion This work shows that HS-SICM is a versatile tool for resolving rapid morphological changes and volume dynamics of adherent living platelets.

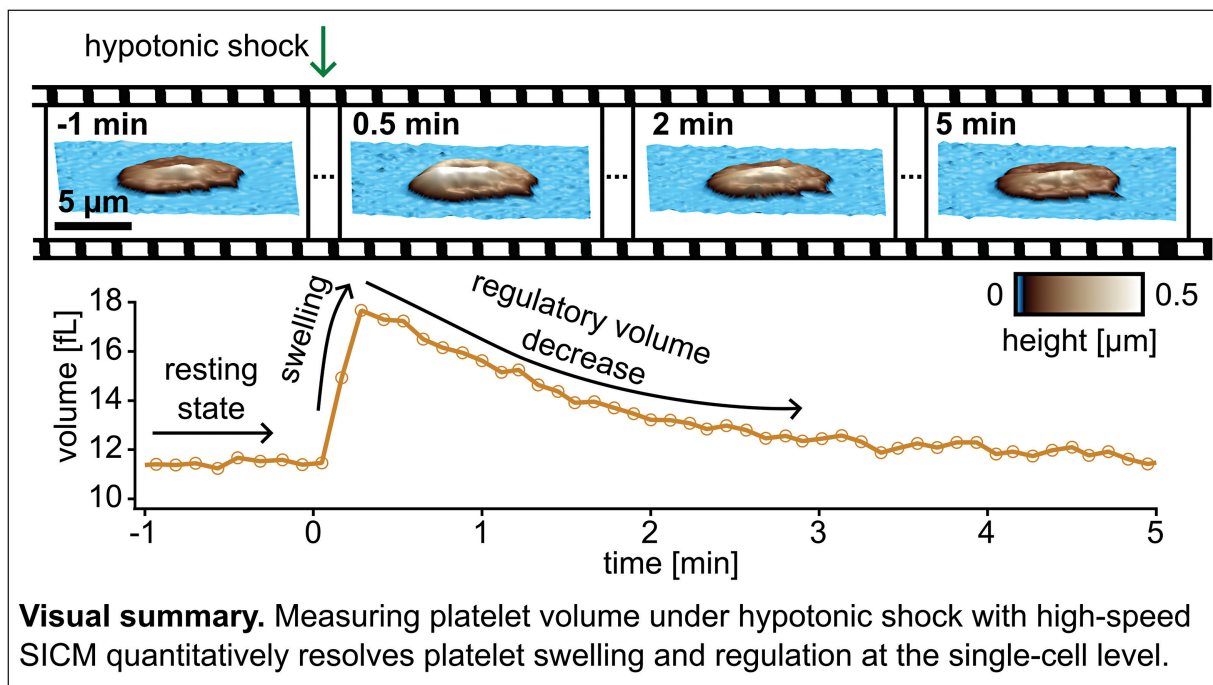
Keywords

- ▶ hypotonic shock
- ▶ platelet volume
- ▶ nonosmotic fraction
- ▶ platelet activation
- ▶ SICM

received
December 21, 2023
accepted after revision
July 28, 2024
accepted manuscript online
August 2, 2024

DOI <https://doi.org/10.1055/a-2378-9088>.
ISSN 0340-6245.

© 2024. The Author(s).
This is an open access article published by Thieme under the terms of the Creative Commons Attribution License, permitting unrestricted use, distribution, and reproduction so long as the original work is properly cited. (<https://creativecommons.org/licenses/by/4.0/>)
Georg Thieme Verlag KG, Rüdigerstraße 14, 70469 Stuttgart, Germany



Introduction

Platelets are one of the three main cellular components present in mammalian blood and play a pivotal role in human physiology, particularly in hemostasis and the intricate process of wound closure. After vessel injury, platelets are activated, adhere to extracellular matrix components such as collagen or fibrinogen, and release chemical signals to attract more platelets to the site of injury.^{1,2} Platelets thereby undergo a shape change to close the injured vessel by agglomeration and formation of a blood clot.^{3,4} Activation can be triggered by various factors,^{4,5} for example, by mechanical or enzymatic stimulation,^{6,7} and uncontrolled platelet activation increases the risk of thrombosis or stroke.^{8,9}

Maintaining a constant platelet volume is critical for correct platelet function.¹⁰ For example, it was shown that water-induced swelling of platelets might promote their activity and thereby initiate thrombosis.¹¹ Therefore, platelets have established an effective volume regulation mechanism (regulatory volume decrease, RVD),¹² based on the passive transport of water by water channels (aquaporins).¹¹ The regulation of platelet volume is associated with a change in the osmolarity of the surrounding medium, which can be an important factor, for example, in blood transfusion.^{13,14} When exposed to a rapid osmolarity change, the platelet changes its volume in response to the osmolarity change of the medium to adapt to the extracellular environment, mediated by an influx or efflux of water through aquaporins in the cell membrane into or out of the cell.^{11,12,15} However, despite its potential significance, the impact of platelet activation on RVD and its role in physiological and pathological processes has not been widely investigated.^{11,16} Single-cell measurements present a significant advantage in this context, as they allow for the characterization of individual platelets, thereby capturing the substantial variance that exists within platelet populations.

Methods to quantify platelet volume such as light transmittance or impedance measurements are limited as they only measure volume qualitatively or only determine the average volume of a platelet population. On the other hand, single-platelet imaging techniques such as atomic force microscopy^{6,17} or fluorescence microscopy^{18,19} might induce unintended platelet activation or often require fixation or fluorescent labeling of the platelets.^{17,20}

We therefore applied high-speed scanning ion conductance microscopy^{21,22} (HS-SICM) to record topography image sequences of individual platelets to investigate the dynamics of water-induced swelling and subsequent volume regulation.^{7,23} As HS-SICM can image live cells with submicrometer resolution without mechanical contact, it is ideal for quantitative assessment of platelet shape and volume²⁴ without the risk of platelet activation.^{7,25} For example, SICM has recently been used to study platelet morphology,²⁶ mechanics,⁷ migration,²⁵ and thrombus formation.²⁷ By optimizing the scanning speed and pixel resolution to measure the volume of individual platelets, we observe rapid volume changes in swelling platelets with a temporal resolution of 7 seconds per frame and a precision of 0.1 fL. We demonstrate that the peak volume and the swelling rate after hypotonic shock directly depend on the osmolarity of the extracellular medium. RVD was suppressed when platelets were investigated in the presence of thrombin, adenosine diphosphate (ADP), or collagen. We also showed that the nonosmotic volume in platelets was reduced in thrombin- or ADP-treated, but not in collagen-treated platelets.

Methods

Human Platelet Isolation and Preparation

All procedures were approved by the institutional ethics committee (273/2018BO2) and comply with the Declaration

of Helsinki. Freshly drawn venous blood of healthy volunteers was used for platelet isolation by using monovettes filled with anticoagulant acid citrate dextrose (at a ratio of 1:4) (04.1926.001, Sarstedt, Nümbrecht, Germany). After centrifugation at $200\times g$ for 20 minutes, platelet-rich plasma was collected and transferred into Tyrode-HEPES buffer solution (136.89 mM NaCl, 2.81 mM KCl, 11.9 mM NaHCO_3 , 1.05 mM MgCl_2 , 0.42 mM NaH_2PO_4 , 5.56 mM D-glucose, 1 g/L bovine serum albumin, 4 mM HEPES), pH 6.5, at a ratio of 1:3. After centrifugation at $880\times g$ for 10 minutes, platelets were carefully resuspended in 1 mL Tyrode-HEPES buffer solution, pH 7.4. The Tyrode-HEPES buffer solution had a standard osmolarity of 295 mOsmol/L and is referred to as “isotonic” in the following.

For HS-SICM measurements, washed platelets were added to a cell culture dish (627160, Greiner Bio-One GmbH, Kremsmünster, Austria). After 10 seconds, nonadherent platelets were removed by carefully washing three times with isotonic Tyrode-HEPES buffer solution, pH 7.4, and adherent platelets were allowed to spread for 10 minutes. Afterwards, the dish was mounted in the HS-SICM setup and HS-SICM measurements were performed at room temperature.

To inhibit the RVD, washed platelets were imaged in isotonic Tyrode-HEPES buffer solution with an increased KCl (+45 mM) and a decreased NaCl (−45 mM) concentration (unchanged osmolarity; this buffer solution is referred to as high K^+ buffer and respective platelets as high K^+ -treated in the following).¹²

To determine the influence of the actin cytoskeleton on the swelling and volume regulation behavior, 50 μM cytochalasin D (cytoD; Cay11330–5, Cayman Chemical Company, Michigan, United States, solved in DMSO) was added to the cell culture dish with adherent platelets during HS-SICM imaging. The solvent DMSO did not affect the platelet volume (► **Supplementary Fig. S4D**, available in the online version).

Activation of platelets was performed by incubating platelets in suspension for 30 seconds with 0.1 U/mL thrombin (T6884–250UN, Sigma-Aldrich, St. Louis, Missouri, United States), or 10 μM ADP (Sigma-Aldrich) before adhesion and spreading.^{28–30} Thrombin or ADP was present at the given concentration during the whole measurement. For platelet activation with collagen,^{31,32} the cell culture dish was incubated with 0.1 mg/mL collagen (Collagen Reagents HORM, Takeda Pharma GmbH, Vienna, Austria) for 1 hour at 37°C. After incubation, the dish was washed three times with Tyrode-HEPES buffer solution, pH 7.4.

A commercial cell counter (impedance measurement principle, Sysmex KX-21N, Sysmex Corporation, Kobe, Japan) was used for the determination of the mean platelet volume (MPV) and the platelet distribution width (PDW) of platelets in whole blood.

HS-SICM Imaging

We used a self-built HS-SICM setup with an electrolyte-filled nanopipette (► **Fig. 1A**). Nanopipettes with inner opening radii of 80 to 100 nm (► **Fig. 1A**, validated by scanning

electron microscopy) were manufactured from borosilicate glass capillaries (Kwik-Fill glass capillaries, World Precision Instruments Inc., Florida, United States) using a CO_2 -laser-based pipette puller (P2000, Sutter Instruments, California, United States). The principle of HS-SICM is described elsewhere in detail.^{21,25,33,34} In brief, a voltage of 250 mV, applied between two Ag/AgCl electrodes, one outside and one inside the pipette, induces an ion current that is dependent on the pipette–surface distance. The three-dimensional topography of the sample surface is acquired by using the ion current as a feedback signal and scanning the pipette over the sample using piezo actuators. The HS-SICM setup was operated in hopping/backstep mode³⁵ with an approach speed of 250 $\mu\text{m/s}$, an ion current trigger of 99.5% of the saturation current for the retraction of the pipette (► **Supplementary Fig. S1A**, available in the online version, dashed lines), and a retract distance of 0.5 μm . The vertical pipette position at the trigger event was stored as the sample height at that location.

To increase the time resolution of HS-SICM imaging, we used masks for scanning only relevant regions (platelet area dilated by 2 μm and 20% random coverage of the substrate area; ► **Supplementary Fig. S1E**, available in the online version). With 40×40 pixels per frame and a standard scan size between 15 and 20 μm , the typical acquisition time was 7 seconds per frame (► **Fig. 1E**).

For obtaining the MPV and the PDW using HS-SICM, the topography of adherent platelets was imaged using $100\times 100\mu\text{m}^2$ scans with a pixel resolution of 150×150 pixels.

Application of Osmotic Shock

To induce a hypotonic shock, the isotonic Tyrode-HEPES buffer solution (isotonic osmolarity of 295 mOsmol/L) was quickly exchanged with hypotonic buffer solution (Tyrode-HEPES buffer solution diluted with pure H_2O [HPLC quality, Fischer Chemical GmbH, Schwerte, Germany] at different volume percentages (10, 20, 30, 40, or 50% pure H_2O of the final solution]), leading to a rapid decrease in osmolarity (265, 236, 206, 177, or 147 mOsmol/L). To induce a hypertonic shock, the isotonic Tyrode-HEPES buffer solution was quickly exchanged with hypertonic buffer solution (Tyrode-HEPES buffer mixed with D-sorbitol [S1876–100G, Sigma Aldrich, Missouri, United States] at different concentrations [59, 118, or 154 mM]), leading to a rapid increase in osmolarity (354, 413, or 447 mOsmol/L) while not affecting platelet viability.³⁶

For normal (untreated) platelets, platelets treated with high K^+ buffer solution, and thrombin-treated platelets, HS-SICM measurements were started 5 minutes before the osmotic shock was induced. For cytoD measurements, adherent platelets were treated with cytoD for 10 minutes before the hypotonic shock was induced (no change in cytoD concentration) and HS-SICM measurements were started 5 minutes before the treatment with cytoD (► **Supplementary Fig. S4C**, available in the online version).

For solution exchange, a 3D-printed (Formlabs 3, Somerville, Massachusetts, United States) cell culture dish holder

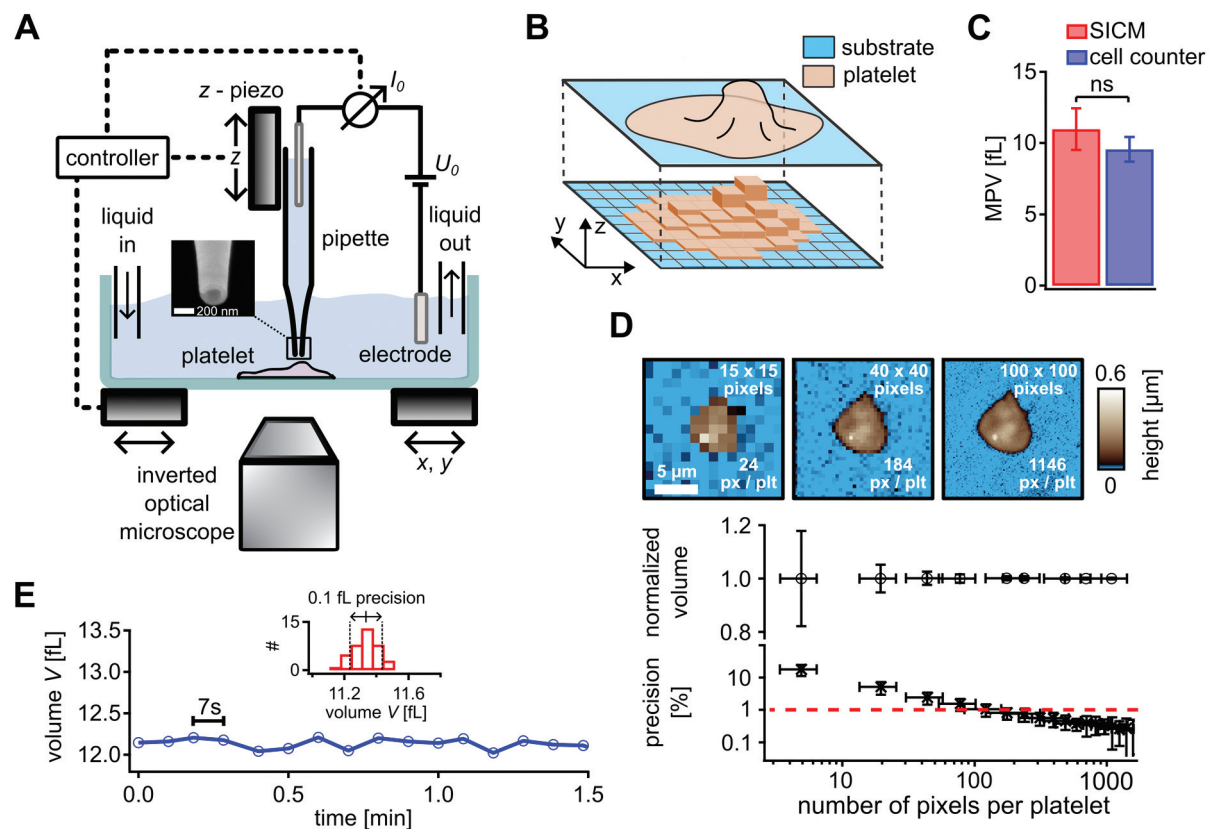


Fig. 1 Platelet topography imaging and volume measurement with HS-SICM. (A) Schematic of the HS-SICM setup using a nanopipette (inset shows scanning electron microscopy image, pipette inner opening radius 90 nm) that is moved relative to the sample in the x -, y -, and z -directions by piezo scanners. A bias voltage U_0 applied between two electrodes induces a distance-dependent ion current I_0 (also see ► **Supplementary Fig. S1A**, available in the online version). The sample buffer solution can be exchanged by using an inlet and an outlet to induce an osmotic shock. (B) Schematic for the calculation of platelet volume from the pixels of a topography image. (C) Average MPV of platelets measured with HS-SICM and a cell counter. (D) HS-SICM topography images (top row) with different pixel resolutions (15×15 , 40×40 , and 100×100 pixels, resulting in 24, 184, and 1,146 pixels per platelet). Normalized volume (middle row) and volume measurement precision (bottom row) averaged over down-sampled platelet images for $N = 26$ platelets versus number of pixels per platelet. A volume measurement precision of 1% (red dashed line) corresponds to approximately 200 pixels per platelet. Error bars show the standard deviation for normalized volume (middle row) and SESD for measurement precision (bottom row). (E) Volume measured for one fixed platelet over time with HS-SICM at 7 seconds per frame. The histogram (inset) shows the volume distribution giving 0.1 fL precision (standard deviation). HS-SICM, high-speed scanning ion conductance microscopy; MPV, mean platelet volume; SESD, standard error of the standard deviation.

with two connections, one for extracting the current buffer solution, and one for adding the exchange buffer solution, was used. HS-SICM imaging was maintained during solution exchange. Although changing the salt concentration of the electrolyte to introduce a hypotonic shock led to a decrease in ion concentration and thus to a decrease in measured ion current (► **Supplementary Fig. S1F**, available in the online version), the quality of HS-SICM images was almost unaffected. In the case of hypertonic shock, no decrease in image quality was observed.

HS-SICM Data Analysis

HS-SICM topography images of platelets were processed and analyzed using Igor Pro 9 (WaveMetrics, Inc., Portland, Oregon, United States). Platelets were identified by a pixel height threshold of $h = 50$ nm, and pixels below this threshold were considered as substrate. All topography images were corrected for tilt (and z -offset by first-order line flattening.³⁷ To calculate the area A of each platelet, the sum of all

pixel areas corresponding to the platelet was formed, $A = \sum_i a_i$. The platelet volume V was calculated by multiplying the area A with the mean height \bar{h} of the platelet, $V = A \cdot \bar{h}$, which is mathematically equivalent to summing up the volumes of all pixels corresponding to the platelet (► **Fig. 1B**).²⁴

For quantifying the influence of the pixel resolution on the measured platelet volume, high-resolution images (giving the “true” volume) were downsampled with systematically varying pipette position offsets. Afterwards, the platelet volumes for the downsampled and flattened images were calculated.

The MPV was calculated as the arithmetic mean of the platelet volumes measured by HS-SICM. The PDW was measured as the width at 20% of the maximum value from log-normal distribution fits (► **Supplementary Fig. S1C, D**, available in the online version).

For investigating the precision of the volume measurement of our HS-SICM system (► **Fig. 1E**), platelets were fixed

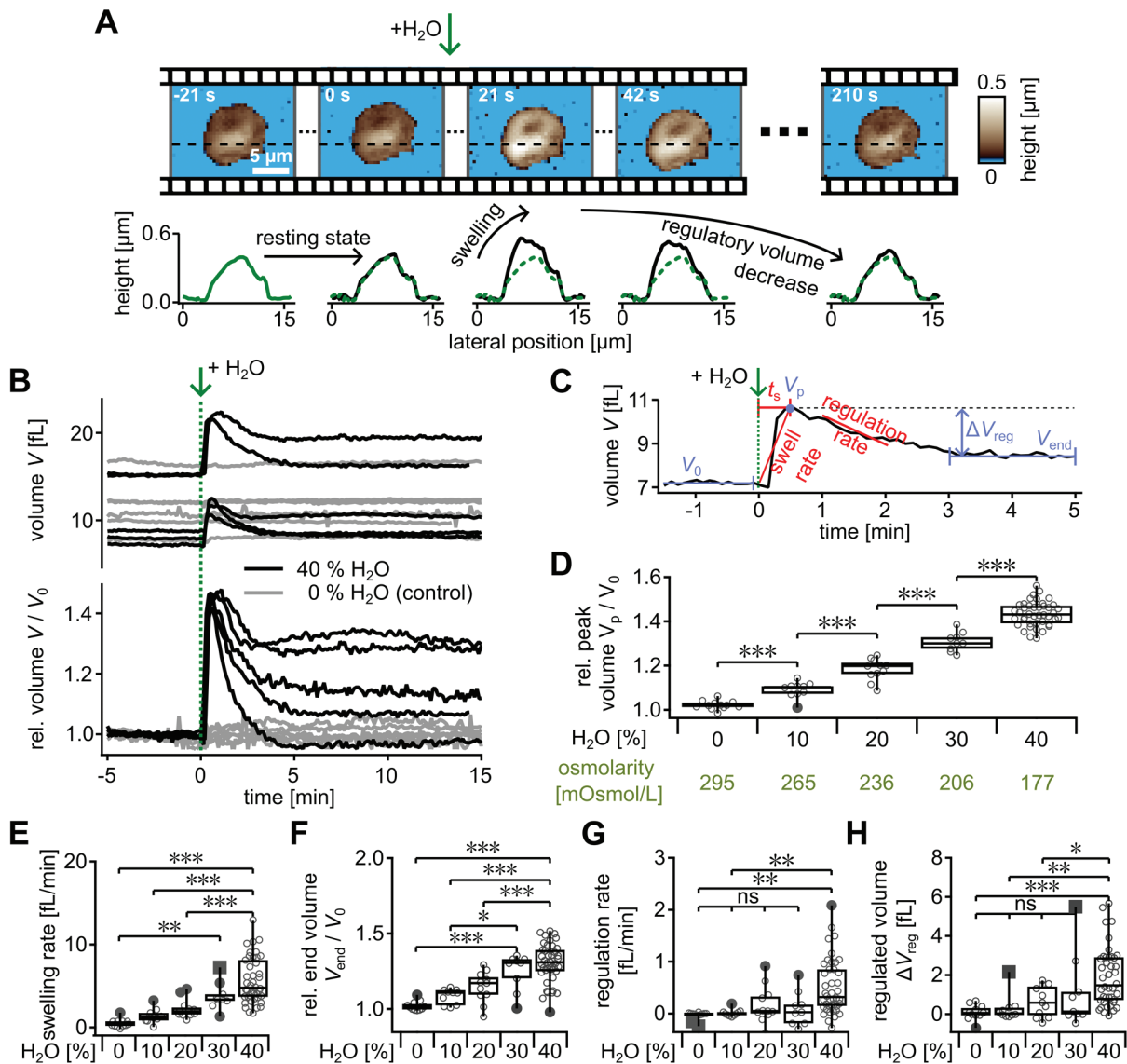


Fig. 2 Quantitative single-platelet volume measurements with HS-SICM, resolving rapid volume dynamics of living platelets after hypotonic shock. (A) Sequence of topography images (top) and corresponding height profiles (bottom). The dashed line corresponds to the platelet before exposure to a hypotonic shock of 40% H_2O at $t = 0$ s. Every third image is shown. The complete image sequence is shown in **► Supplementary Fig. S2A** (available in the online version) and in **► Supplementary Video 1** (available in the online version). The hypotonic shock induces a rapid height increase (swelling) of the platelet, followed by a slower height decrease (regulatory volume decrease). (B) Time dynamics of the volume (top) and the volume relative to the initial volume V_0 (bottom) of individual platelets exposed to a hypotonic shock at $t = 0$ with 40% H_2O (black curves) or 0% H_2O (gray curves, control). (C) Representative volume vs. time curve showing the definitions of the initial volume V_0 , the peak volume (V_p), the regulated volume (ΔV_{reg}), the final volume (V_{end}), the swelling time t_s , the swelling rate, and the regulation rate. (D) Relative peak volume V_p/V_0 after a hypotonic shock with varying osmolarity. (E) Swelling rate, (F) relative end volume V_{end}/V_0 , and (G) regulation rate for a hypotonic shock with varying osmolarity. (H) Regulated volume ΔV_{reg} of platelets after a hypotonic shock with varying osmolarity. Number of platelets (D–H): $N = 12$ (0% H_2O), 10 (10%), 11 (10%), 9 (30%), and 42 (40%). HS-SICM, high-speed scanning ion conductance microscopy.

in 2% formaldehyde for 10 minutes at room temperature. Then, $N = 5$ fixed platelets were imaged over time (at least 20 minutes).

For all time-dependent measurements, $t = 0$ was defined as the time of the hypotonic shock. The time interval before the hypotonic shock [–5 minutes; 0 minute] was used for the calculation of the initial volume V_0 (average volume before the hypotonic shock). The relative volume was then calculated as V/V_0 with the initial volume V_0 (**► Fig. 2C**). The swelling time t_s (**► Fig. 2C**) was determined

by calculating the time between the hypotonic shock (green arrow at $t = 0$) and the peak volume V_p . The platelet swelling rate was defined as $\frac{V_p - V_0}{t_s}$. The regulation rate was determined as the slope of the volume between $t = 1$ and 2 min after the peak volume V_p by applying a line fit (**► Fig. 2C**). The end volume V_{end} was defined as the average volume between $t = 3$ min and 5 min after the hypotonic shock. The regulated volume was calculated as $\Delta V_{\text{reg}} = V_p - V_{\text{end}}$. Hence, for $\Delta V_{\text{reg}} \sim 0$, a platelet was interpreted as nonregulating.

The platelet-to-platelet variation of the RVD was calculated as the standard deviation σ of the relative end volume V_{end}/V_0 with standard error of the standard deviation (SESD) $= \frac{\sigma}{\sqrt{2 \cdot (N-1)}}$, with number of platelets N .

To determine the nonosmotic fraction of the platelets, we used the Boyle–van't Hoff relationship³⁸ for cells under osmotic conditions, which assumes a linear correlation between the (relative) cell volume and the inverse tonicity^{12,39} Ψ (here: ratio of the isotonic osmolarity and the hypo-/hypertonic osmolarity). For individual platelets, two data points were available: $V_0/V_0 = 1$ at $\Psi = 1$ before the osmotic shock, and V_p/V_0 at the given Ψ after the osmotic shock (before regulation). We plotted the relative platelet volumes as a function of Ψ and applied a line fit to the data points. The value of the fit at $\Psi = 0$ gives the osmotically inactive, nonosmotic fraction of the platelets.¹² For the calculation of the nonosmotic fraction of the platelet population, the line fit was applied to the averaged volumes at the given Ψ .

Statistical Analysis

Statistical tests were performed using Igor Pro 9 (Wave-Metrics, Inc., Portland, Oregon, United States). Box plots show the median and the lower and upper quartiles. For the comparison between two groups, Student's t -test was used. For comparison between three or more groups, Tukey's range test was used. Variances were tested with the F-test for significance. The results were considered as significantly different for $p \leq 0.05$ (*), $p \leq 0.01$ (**), and $p \leq 0.001$ (***), and as not significantly different (ns) for $p > 0.05$. Platelets from three to eight independent donors were measured.

Results and Discussion

Optimization of Fast Volume Measurements with HS-SICM

The topography of individual adherent, spread platelets was imaged using HS-SICM (►Fig. 1A). Platelets usually had a spread-out morphology with a flat lamellipodium at the outer regions and a higher platelet body at the center (►Supplementary Fig. S1B, available in the online version). In a topography image, the platelet volume corresponds to the sum of the effective volume of all pixels of the platelet (►Fig. 1B). To verify that SICM accurately measures platelet volume, we compared the MPV of three different donors as obtained from SICM topography images with the MPV measured with a conventional cell counter as “gold standard,” revealing no significant difference (►Fig. 1C and ►Supplementary Fig. S1C [available in the online version]). However, within individual donors, there was a trend for slightly larger MPV and PDW with SICM compared with the cell counter (►Supplementary Fig. S1D, available in the online version). This discrepancy could likely arise from the difference in measurement conditions, since we measured adherent washed platelets with SICM as opposed to platelets from whole blood in solution with the cell counter.

The measurement speed of SICM is dependent on numerous factors and the acquisition of a topography image typically

takes several minutes,³⁵ limiting the ability to measure rapid morphological changes of individual human platelets. The acquisition time in HS-SICM in the hopping mode is proportional to the number of pixels of the image. At a low number of pixels per image, the acquisition time is short, but the image resolution is low due to a high degree of pixelation of the platelet (►Fig. 1D, left image), making volume measurements less precise. To find the optimum number of pixels per platelet for a given volume precision, we recorded a high-resolution image (200×200 pixels) of a platelet and progressively down-sampled this image to generate lower resolution images (100×100 , 40×40 , and 15×15 pixels; ►Fig. 1D, top; also see the Methods section). From each of these images, we measured the platelet volume (normalized by the “true” platelet volume from the respective high-resolution image). Repeating this process for 26 images of different platelets allowed us to plot the average of the measured normalized volumes and the average precision of the volume measurements as a function of the number of pixels per platelet (►Fig. 1D, center and bottom). While the average normalized volume stayed constant for an increasing number of pixels per platelet (►Fig. 1D, center), the precision of that measurement improved (►Fig. 1D, bottom). For a volume measurement precision of 1%, we need about $n = 200$ pixels per platelet (►Fig. 1D, bottom, red dashed line). For a typical platelet area A , this corresponds to a required pixel size of $s_{\text{px}} = \sqrt{\frac{A}{n}}$.

Assuming a circular platelet of diameter d , the required pixel size is $s_{\text{px}} = \sqrt{\frac{\pi}{4n}} \cdot d = 0.063 d$, which amounts to $d/s_{\text{px}} = 16$ pixels across the platelet. For a typical platelet diameter of $7 \mu\text{m}$ (►Supplementary Fig. S1B, available in the online version), the required pixel size is $s_{\text{px}} = 440 \text{ nm}$ (for 1% precision in the platelet volume measurement). In our experiments, we therefore chose an image resolution of 40×40 pixels with a scan size of 15 to $20 \mu\text{m}$.

To further speed up the imaging, we reduced the number of pixels acquired on the substrate around the platelet by computing a dynamic mask around the platelet (►Supplementary Fig. S1E, available in the online version, images). These optimizations facilitated a reduction in acquisition time by a factor of approximately 2.5 in this example (►Supplementary Fig. S1E, available in the online version, right). As a result, we were able to capture rapid topography and volume changes of individual living platelets with acquisition times of down to 7 seconds per frame (►Fig. 1E and ►Supplementary Fig. S2A [available in the online version]) (comparable with values reported in other HS-SICM publications^{40,41}) and with a precision of typically 0.1 fL (►Fig. 1E, inset) (which reflects the 1% precision from the pixelation set above).

Platelet Swelling after Hypotonic Shock

In contrast to previous studies, which measured suspended platelet volume changes in solution, averaged over a whole population of platelets, or performed only qualitative measurements,^{14,15,42} our approach with HS-SICM allows capturing quantitative, time-lapse volume changes of adherent platelets undergoing hypotonic shock. Platelets showed a rapid swelling

with an increase in platelet height after hypotonic shock (► **Fig. 2A**, ► **Supplementary Fig. S2A** [available in the online version]), and ► **Supplementary Video 1** [available in the online version]). Subsequently, the height slowly decreased again toward almost the initial height (RVD; ► **Fig. 2A**). From such image sequences, we measured the platelet volume V (► **Fig. 2B**, top) and the volume relative to the initial volume V_0 (► **Fig. 2B**, bottom) as a function of time. The volume of platelets exposed to a hypotonic shock of 40% H₂O rapidly increased within seconds after the shock (► **Fig. 2B**, black curves). Within ≈1 minute after the hypotonic shock, the volume started to decrease again and became constant at ≈5 minutes. Platelets without a hypotonic shock did not show any significant increase in volume (► **Fig. 2B**, gray curves). Platelets during hypotonic shock with lower H₂O percentages generally showed a weaker volume change but a similar time behavior (► **Supplementary Fig. S2B–D**, available in the online version). These volume dynamics can be parameterized (► **Fig. 2C**) as the initial volume V_0 before the hypotonic shock, the peak volume V_p reached at the swelling time t_s after the hypotonic shock, the end volume V_{end} , the regulated volume $\Delta V_{reg} = V_p - V_{end}$, the swelling rate, and the regulation rate.

Supplementary Video 1

Image sequence of platelet topography using HS-SICM with an acquisition time of 7 s per frame. A hypotonic shock with 40% H₂O was induced at $t = 5$ min. Online content including video sequences viewable at: <https://www.thieme-connect.com/products/ejournals/html/10.1055/a-2378-9088>.

The relative peak volume V_p/V_0 increased significantly for an increasing H₂O percentage and hence for decreasing osmolarity (► **Figs. 2D** and ► **Supplementary Fig. S2B–D** [available in the online version]). The swelling rate also increased with the H₂O percentage (► **Fig. 2E**). In contrast, the swelling time did not depend on the H₂O percentage and was therefore independent of the osmolarity (► **Supplementary Fig. S3A**, available in the online version). This indicates that a hypotonic shock with a larger osmotic change induces a larger water influx into the platelet, which supports the assumption that the volume increase in platelets is driven by diffusion.^{43,44} This assumption was further upheld by the roughly linear correlation ($r = 0.66 \pm 0.091$, $p = 3.0410^{-10}$) between the initial platelet volume V_0 (as a measure of platelet size) and the swelling rate (► **Supplementary Fig. S3B**, available in the online version), showing that larger platelets with a larger surface area can take up larger amounts of H₂O per time. Consequently, the swelling rate of platelets showed a significant size-dependency for a hypotonic shock with 40% H₂O when comparing small ($V_0 < 12$ fl) and large ($V_0 \geq 12$ fl) platelets (► **Supplementary Fig. S3C**, available in the online version, left). In contrast, the regulation rate did not depend on platelet size (► **Supplementary Fig. S3C**, available in the online version,

right). For better comparison of the end volume V_{end} (volume plateau after regulation) between differently sized platelets and different H₂O percentages, we investigated the relative end volume V_{end}/V_0 , showing a significant increase with H₂O percentage (► **Fig. 2F**).

The regulation rate was significantly increased ($p = 0.0012$, compared with control) only after hypotonic shock with 40% H₂O (► **Fig. 2G**). Thus, both the regulated volume ΔV_{reg} (► **Fig. 2H**) and the relative regulated volume $\Delta V_{reg}/V_0$ (► **Supplementary Fig. S3D**, available in the online version) were significantly ($p = 0.00098$, $p = 0.00012$, respectively, compared with control) increased only after a hypotonic shock with 40% H₂O and were much smaller for 30% H₂O or lower, indicating that RVD is more pronounced at a hypotonic shock with lower osmolarity.⁴⁵ In the following, we therefore used 40% H₂O to induce a hypotonic shock. For comparison, platelets exposed to hypertonic shock rapidly shrank but did not show a notable regulatory volume increase (RVI; ► **Supplementary Fig. S2E**, available in the online version). This aligns with previous findings that platelets, among other cell types, respond to hypertonic shrinking with activation of Na⁺/H⁺ exchange but do not exhibit a detectable RVI.¹² This behavior may be explained by different ion channels involved in RVD and RVI. In RVD, mainly K⁺ and Cl⁻ are secreted,⁴⁶ leading to an efficient change of the intracellular osmolarity by water efflux, whereas in RVI, mainly the Na⁺/H⁺ exchanger is activated, which might decrease the net gain of osmolytes in RVI.⁴⁷ However, some cell types can exhibit an effective RVI after hypertonic shock, but the reason for the different RVI behaviors is yet unknown.⁴⁸

The swelling induced by the hypotonic shock primarily caused an increase in platelet height, while the platelet area did not significantly change (► **Supplementary Fig. S3E**, available in the online version). Interestingly, for a hypotonic shock with 80% H₂O, which led to an average relative peak volume of $V_p/V_0 = 2.32$, the formation of a filopodium could be observed within minutes after the hypotonic shock (► **Supplementary Fig. S3F, G** [available in the online version]; also see ► **Supplementary Videos 2** and **3** [available in the online version]), which is a possible indicator of platelet apoptosis.⁶ The absence of filopodia at 40% H₂O and below supports the assumption that platelet viability is not notably decreased by hypotonic shocks with lower osmolarities and that platelets can swell and regulate their volume without apoptosis.¹²

Supplementary Video 2

Image sequence of platelet topography using HS-SICM with an acquisition time of 7 s per frame. A hypotonic shock with 80% H₂O was induced at $t = 5$ min, leading to the formation of a filopodium. Online content including video sequences viewable at: <https://www.thieme-connect.com/products/ejournals/html/10.1055/a-2378-9088>.

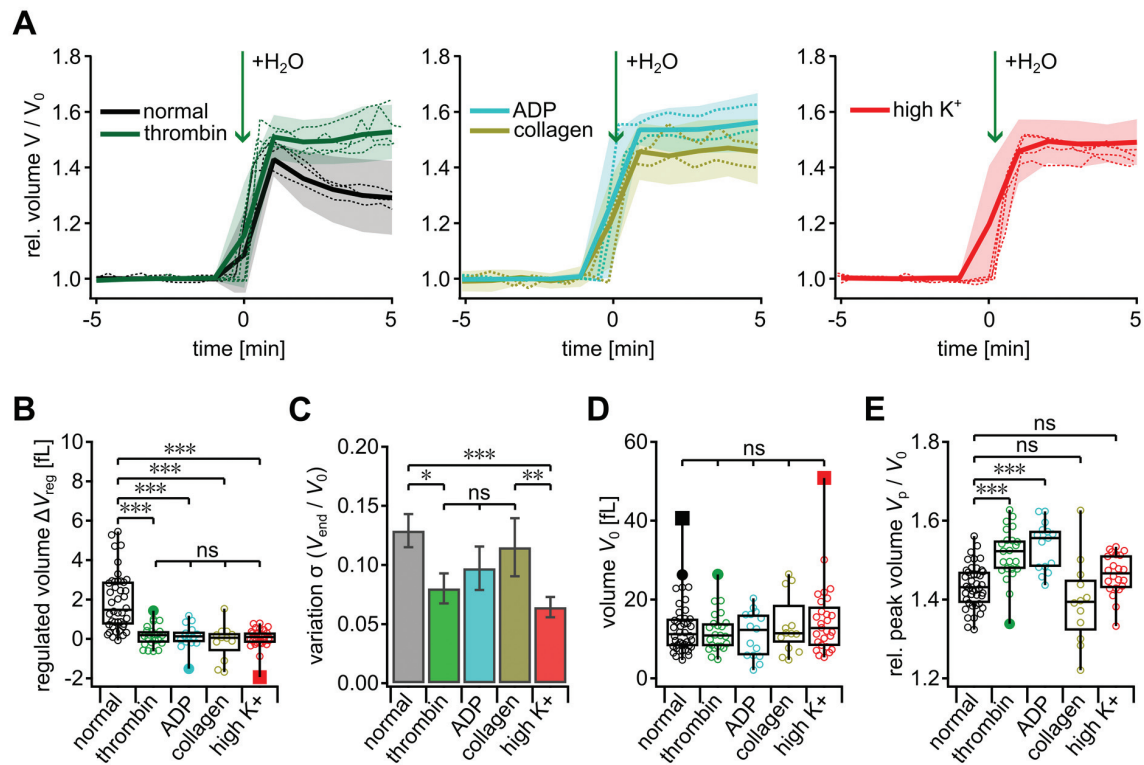


Fig. 3 RVD of individual platelets after a hypotonic shock with 40% H₂O. (A) Relative volume vs. time of representative individual platelets (dashed lines) during a hypotonic shock for different platelet treatments. Solid lines and shaded areas represent the mean and standard deviation, respectively, of all measured platelets. (B) Regulated volume ΔV_{reg} for normal (untreated), thrombin-treated, ADP-treated, collagen-treated, and high K⁺-treated platelets. (C) Variation σ of the relative end volume V_{end}/V_0 . Error bars show the SESD. (D) Initial volume V_0 and (E) relative peak volume V_p/V_0 for different platelet treatments. Significance in (C) was determined using the F-test. Number of cells (B–E): $N = 43$ (normal), 23 (thrombin), 15 (ADP), 12 (collagen), and 28 (high K⁺). SESD, standard error of the standard deviation; RVD, regulatory volume decrease.

Supplementary Video 3

Image sequence of platelet topography using HS-SICM with an acquisition time of 7 s per frame. A hypotonic shock with 80% H₂O was induced at $t = 5$ min, leading to the formation of a filopodium. Online content including video sequences viewable at: <https://www.thieme-connect.com/products/ejournals/html/10.1055/a-2378-9088>.

RVD of Platelets Is Suppressed after Platelet Activation

To investigate the influence of platelet activation on the RVD, we first used thrombin as a potent platelet activator.^{7,23} While normal (untreated) platelets showed a normal RVD after a hypotonic shock with 40% H₂O (► Fig. 3A, left, black traces), as already reported above, thrombin-treated platelets showed no notable RVD after the hypotonic shock, but remained at a constantly high volume (► Fig. 3A, left, green traces). Consequently, the regulated volume ΔV_{reg} of thrombin-treated platelets was significantly reduced ($p = 1.8910^{-8}$) compared with normal platelets (► Fig. 3B).

Taking advantage of the single-platelet resolution of HS-SICM, we calculated the platelet-to-platelet variation σ of the

RVD as a function of time (► Fig. 3A, shaded areas) and the standard deviation σ of the relative end volume V_{end}/V_0 (► Fig. 3C). For thrombin-treated platelets, the platelet-to-platelet variation σ was significantly reduced ($p = 0.019$) compared with normal platelets, which indicates a more homogenous behavior of the platelets after hypotonic shock.

To investigate whether activation generally suppresses RVD in platelets, we further used ADP^{49,50} and collagen³² (► Supplementary Fig. S4A, available in the online version) on platelets undergoing hypotonic shock (► Fig. 3A, center, light blue and yellow traces). Like thrombin-treated platelets, ADP and collagen both suppressed RVD after hypotonic shock with 40% H₂O as indicated by a constant high relative volume after hypotonic shock (► Fig. 3A). Consequently, the regulated volume ΔV_{reg} was significantly ($p = 2.7510^{-5}$ and $p = 7.8810^{-6}$, respectively) reduced compared with normal platelets (► Fig. 3B). Further, the platelet-to-platelet variation σ of the RVD for ADP- and collagen-treated platelets was also smaller and similar to thrombin-treated platelets (► Fig. 3C). Therefore, we propose that activation inhibits RVD in adherent platelets.

For comparison, we measured platelets in the presence of a high K⁺ buffer, which is known to effectively inhibit the RVD.¹² As expected, platelets exposed to high K⁺ buffer did not show a strong RVD (► Fig. 3A, right, red curves) and their regulated volume ΔV_{reg} was close to zero, significantly

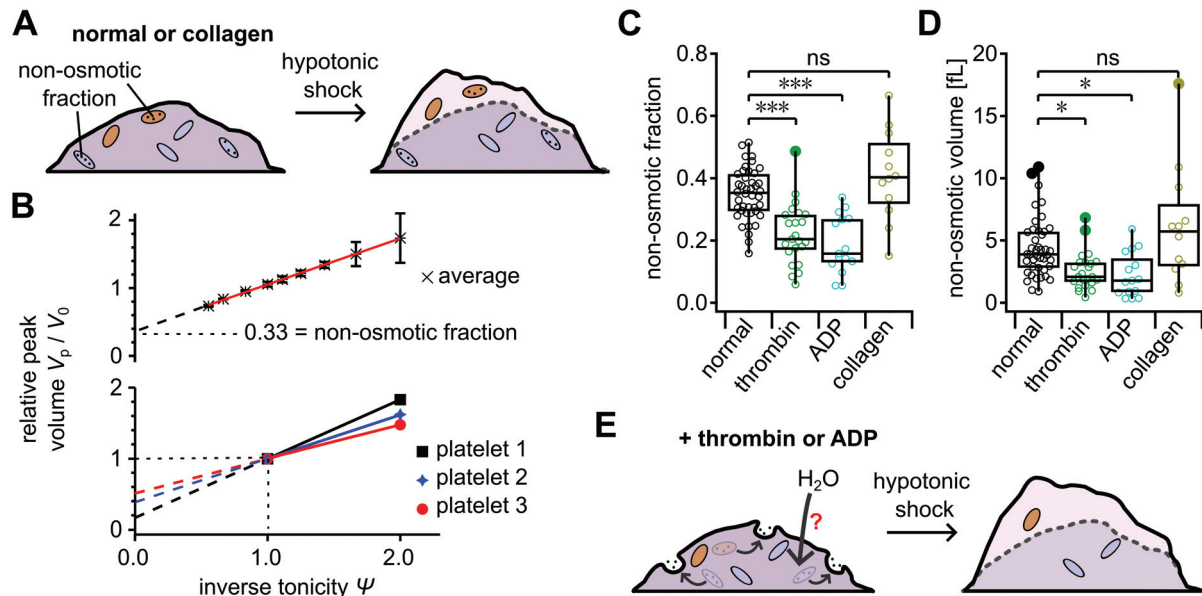


Fig. 4 Determination of the nonosmotic fraction of swelling platelets with HS-SICM. (A) Schematic of the behavior of the nonosmotic fraction during hypotonic shock of normal or collagen-treated platelets. (B) Relative peak volume V_p/V_0 versus the inverse tonicity Ψ averaged for many normal platelets (top) and for three individual normal platelets (bottom). Following the Boyle–van’t Hoff relationship, the osmotically inactive, nonosmotic volume fraction is given by the y-intercept of the line. (C) Nonosmotic fraction and (D) nonosmotic volume of normal, thrombin-, ADP-, and collagen-treated platelets. (E) Schematic of the possible action of thrombin or ADP on a platelet before and after hypotonic shock. The nonosmotic volume is denoted by the colored objects inside the platelet. Thrombin- and ADP-induced vesical fusion with the platelet membrane is indicated by small arrows. Number of cells (C, D): $N = 82$ (B); $N = 42$ (normal), 23 (thrombin), 15 (ADP), and 12 (collagen). HS-SICM, high-speed scanning ion conductance microscopy.

smaller ($p = 4.2410^{-10}$) than for normal platelets and similar to activated platelets (► Fig. 3B). Importantly, the platelet-to-platelet variation was also smaller than for normal platelets ($p = 0.00028$). During RVD, the efflux of K^+ and Cl^- ions leads to an efflux of water and a decrease in cell volume,^{36,51} which is in line with the reduced efficiency of RVD in the presence of high K^+ solutions.^{12,52} As the corresponding ion channels are also involved in platelet activation,^{46,53} treatment with thrombin, ADP, or collagen could possibly reduce the ability of the ion channels in mediating RVD. Additionally, the absence of RVD in activated platelets may be further attributed to a change in the actin cytoskeleton and in ion channel and transporter activity.^{12,54–57}

As activation is known to affect the platelet cytoskeleton, we also investigated a possible influence of the cytoskeleton on the RVD, as it is known for many cell types.^{58,59} We therefore treated adherent platelets with 50 μ M cytoD during HS-SICM imaging to inhibit actin polymerization (► Supplementary Fig. S4B, available in the online version).^{58,60} This led to a slight volume increase (► Supplementary Fig. S4C, available in the online version), indicating reduced internal stress from active actin cytoskeleton remodeling during adhesion and spreading.^{61–63} Despite this, the RVD was still present and the regulated volume ΔV_{reg} , the platelet-to-platelet variation σ , the initial volume V_0 , and the relative peak volume V_p/V_0 after hypotonic shock with 40% H_2O were similar to normal platelets (► Supplementary Fig. S4E–H, available in the online version). Therefore, RVD in platelets appears to be independent of the actin cytoskeleton, unlike for other cell types, where an intact actin cytoskeleton is crucial for effective RVD.^{58,59,64}

The Nonosmotic Fraction of Platelets Varies Depending on the Activation Agonist

The initial platelet volume V_0 was identical for all treatments (► Fig. 3D). The relative peak volume V_p/V_0 was significantly different for platelets treated with thrombin or ADP ($p = 0.00013$, and $p = 2.7510^{-5}$, respectively; ► Fig. 3E). In contrast, collagen-treated platelets had a similar relative peak volume V_p/V_0 to normal platelets (► Fig. 3E).

This observation prompted us to investigate the nonosmotic volume of platelets. Similar to other mammalian cells, the cytoplasm of platelets contains both osmotically active and inactive components^{43,65} (► Fig. 4A). Plotting the average relative peak volume V_p/V_0 versus the inverse tonicity (► Fig. 4B, top) and using the Boyle–van’t Hoff relationship³⁸ for cells under different osmotic conditions (see the Methods section) allowed us to extract the nonosmotic fraction as the intercept of the extrapolated line fit with the y-axis: 0.33 ± 0.01 . This value is consistent with the literature for platelets¹² and other cells.⁶⁶ Moreover, we were able to determine the nonosmotic fraction of individual platelets (► Fig. 4B, bottom, intercepts with the y-axis). We observed a significant variation in the nonosmotic fraction among individual platelets, ranging between 0.2 and 0.5 (► Fig. 4C, normal) and between 1 and 12 fL (► Fig. 4D, normal). The nonosmotic volume was found to be proportional to the initial volume V_0 (► Supplementary Fig. S5A, available in the online version). Consequently, the nonosmotic fraction was independent of the initial volume V_0 (► Supplementary Fig. S5B, available in the online version).

For thrombin- or ADP-induced activation, both the nonosmotic fraction ($p = 1.423610^{-5}$, $p = 2.234510^{-6}$, respectively) and the nonosmotic volume ($p = 0.0319$, $p = 0.0274$, respectively) were significantly decreased by approximately 42% (thrombin) and 55% (ADP) compared with normal platelets (►Fig. 4C, D). For collagen-induced activation, in contrast, the nonosmotic fraction and volume were unchanged (►Fig. 4A, C, D). These observations are consistent with previous studies that have demonstrated that thrombin^{67,68} and ADP^{28,30} induce a “release reaction” in platelets, causing various soluble and nonsoluble components, for example, granule fractions, serotonin, or platelet factor 4, to be released into the extracellular space, while collagen activation prompts the release of mostly soluble compounds.³¹ Thrombin and ADP trigger the release of Ca^{2+} into the cytosol, promoting vesicle fusion with the membrane (►Fig. 4E, small arrows).^{69,70} The extracellular release of Ca^{2+} is typically mediated by the $\text{Na}^+/\text{Ca}^{2+}$ exchanger, which is activated as a secondary response to elevated intracellular Ca^{2+} levels.^{11,53,71}

As the measured initial volume V_0 was similar for normal, thrombin- and ADP-treated platelets (►Fig. 3D), we hypothesize that the release of nonosmotic volume⁷² into the extracellular space by vesicle fusion is accompanied by an influx of water into the platelet to maintain the initial volume (►Fig. 4E). A possible explanation for this phenomenon could be the relief of membrane tension by exocytotic vesicle fusion, which could trigger water influx (►Fig. 4E, large arrow).⁷³

Conclusion

We investigated dynamic volume changes of individual human platelets by topography imaging with HS-SICM. This technique permits noninvasive imaging of living cells at submicrometer spatial resolution and a time resolution on the second scale without mechanical interaction with the sample. We optimized the time resolution of HS-SICM imaging for precise volume measurement, linking a threshold of 200 pixels per platelet to a measurement precision of 1% (►Fig. 1D). The imaging speed was further increased by reducing the number of pixels in the background, leading to an acquisition time of 7 seconds per frame and a volume measurement precision of 0.1 fl (►Fig. 1E).

We used our HS-SICM setup to investigate the behavior of adherent and spread platelets in response to a hypotonic shock (►Fig. 2). The platelet volume rapidly increased after hypotonic shock and was slowly regulated back toward its initial value. The relative peak volume of platelets showed a significant volume increase with an increase in H_2O percentage, and hence a decrease in osmolarity. Moreover, the swelling rate but not the swelling time depended on the osmolarity. A pronounced RVD was observed after a hypotonic shock with 40% H_2O (►Fig. 2H). Contrary to some other mammalian cell types,⁵⁸ RVD in platelets did not depend on the actin cytoskeleton.⁷⁴ We found that platelet activation by thrombin, ADP, or collagen significantly reduced RVD of individual platelets (►Fig. 3), like RVD inhibition with high K^+ .

The platelet peak volume V_p followed the Boyle–van’t Hoff relationship for different osmotic conditions, from which we

quantitatively determined the nonosmotic fraction of individual platelets as 0.33 on average (►Fig. 4), in good agreement with the literature. In contrast to collagen-treated platelets, thrombin- and ADP-treated platelets showed a significant decrease (42 and 55%, respectively) in the nonosmotic fraction and volume (►Fig. 4C, D), which has not been shown on a single-cell level before.

In conclusion, this work shows that HS-SICM is a versatile tool for resolving rapid morphological changes and volume dynamics of adherent living platelets. To further investigate and correlate vesicle fusion with our observations, future studies could utilize capacitance measurements to provide insights into potential volume changes induced by thrombin or ADP during vesicle fusion and the associated membrane surface changes.⁷¹ Future studies could employ SICM for measuring mechanical⁷⁵ and electrical⁷⁶ properties of adherent platelets, making SICM a valuable addition to well-established technologies for measurement of suspended platelets. Such studies could provide new insights into the links between platelet volume regulation mechanisms, mechanics, membrane function, and compartmentalization in health and disease.

What is known about this topic?

- Platelets show a regulatory volume decrease after hypotonic shock.
- Measurements of platelet volume regulation have been performed qualitatively on large platelet ensembles.

What does this paper add?

- Quantitative, time-resolved measurement of the volume regulation after hypotonic shock of individual platelets using HS-SICM.
- The regulatory volume decrease is suppressed in activated platelets.
- Determination of the nonosmotic fraction of individual platelets via the Boyle–van’t Hoff relationship.
- Thrombin- and ADP-activated platelets show a decreased nonosmotic fraction.

Authors’ Contribution

K.K., J.S., M.G., J.R., and T.S. designed the study. K.K. performed the experiments, analyzed data, and drafted the manuscript. All authors interpreted data, discussed results, and revised the manuscript.

Funding

This work was funded by the Deutsche Forschungsgemeinschaft (DFG, German Research Foundation)—Projekt-nummer 335549539/GRK2381 and Projektnummer 374031971-TRR 240. We acknowledge support by Open Access Publishing Fund of the University of Tübingen.

Conflict of Interest

None declared.

References

- 1 Nurden AT. Platelets, inflammation and tissue regeneration. *Thromb Haemost* 2011;105(Suppl 1):S13–S33
- 2 Thomas MR, Storey RF. The role of platelets in inflammation. *Thromb Haemost* 2015;114(03):449–458
- 3 Holinstat M. Normal platelet function. *Cancer Metastasis Rev* 2017;36(02):195–198
- 4 White JG, Leistikow EL, Escolar G. Platelet membrane responses to surface and suspension activation. *Blood Cells* 1990;16(01):43–70, discussion 70–72
- 5 Rohlfing AK, Kolb K, Sigle M, et al. ACKR3 regulates platelet activation and ischemia-reperfusion tissue injury. *Nat Commun* 2022;13(01):1823
- 6 Posch S, Neundlinger I, Leitner M, et al. Activation induced morphological changes and integrin α IIb β 3 activity of living platelets. *Methods* 2013;60(02):179–185
- 7 Rheinlaender J, Vogel S, Seifert J, et al. Imaging the elastic modulus of human platelets during thrombin-induced activation using scanning ion conductance microscopy. *Thromb Haemost* 2015;113(02):305–311
- 8 Gasparyan AY, Ayvazyan L, Mikhailidis DP, Kitas GD. Mean platelet volume: a link between thrombosis and inflammation? *Curr Pharm Des* 2011;17(01):47–58
- 9 Fitzgerald DJ, Roy L, Catella F, Fitzgerald GA. Platelet activation and atherothrombosis. *N Engl J Med* 1986;315:983–989
- 10 Colkesen Y, Muderrisoglu H. The role of mean platelet volume in predicting thrombotic events. *Clin Chem Lab Med* 2012;50(04):631–634
- 11 Agbani EO, Williams CM, Li Y, et al. Aquaporin-1 regulates platelet procoagulant membrane dynamics and in vivo thrombosis. *JCI Insight* 2018;3(10):e99062
- 12 Livne A, Grinstein S, Rothstein A. Volume-regulating behavior of human platelets. *J Cell Physiol* 1987;131(03):354–363
- 13 Odink J. Platelet preservation. II. The response of human platelet suspensions to hypotonic stress. *Thromb Haemost* 1976;36(01):182–191
- 14 Kim BK, Baldini MG. The platelet response to hypotonic shock. Its value as an indicator of platelet viability after storage. *Transfusion* 1974;14(02):130–138
- 15 Lee JS, Agrawal S, von Turkovich M, Taatjes DJ, Walz DA, Jena BP. Water channels in platelet volume regulation. *J Cell Mol Med* 2012;16(04):945–949
- 16 Szirmai M, Sarkadi B, Szász I, Gárdos G. Volume regulatory mechanisms of human platelets. *Haematologia (Budap)* 1988;21(01):33–40
- 17 Fritz M, Radmacher M, Gaub HE. In vitro activation of human platelets triggered and probed by atomic force microscopy. *Exp Cell Res* 1993;205(01):187–190
- 18 Errington RJ, White NS. Measuring dynamic cell volume in situ by confocal microscopy. *Methods Mol Biol* 1999;122:315–340
- 19 Klaverkamp J, Völkl KP. Maintenance of platelet viability after platelet-labeling with fluorescein isothiocyanate. *Haemostasis* 1984;14(04):337–346
- 20 Nakamura T, Ariyoshi H, Kambayashi J, et al. Effect of low concentration of epinephrine on human platelet aggregation analyzed by particle counting method and confocal microscopy. *J Lab Clin Med* 1997;130(03):262–270
- 21 Hansma PK, Drake B, Marti O, Gould SAC, Prater CB. The scanning ion-conductance microscope. *Science* 1989;243(4891):641–643
- 22 Korchev YE, Bashford CL, Milovanovic M, Vodyanoy I, Lab MJ. Scanning ion conductance microscopy of living cells. *Biophys J* 1997;73(02):653–658
- 23 Seifert J, Rheinlaender J, Lang F, Gawaz M, Schäffer TE. Thrombin-induced cytoskeleton dynamics in spread human platelets observed with fast scanning ion conductance microscopy. *Sci Rep* 2017;7(01):4810
- 24 Korchev YE, Gorelik J, Lab MJ, et al. Cell volume measurement using scanning ion conductance microscopy. *Biophys J* 2000;78(01):451–457
- 25 Seifert J, Rheinlaender J, von Eysmond H, Schäffer TE. Mechanics of migrating platelets investigated with scanning ion conductance microscopy. *Nanoscale* 2022;14(22):8192–8199
- 26 Liu X, Li Y, Zhu H, et al. Use of non-contact hopping probe ion conductance microscopy to investigate dynamic morphology of live platelets. *Platelets* 2015;26(05):480–485
- 27 Nестеle JA, Rohlfing AK, Dicenta V, et al. Characterization of GPVI- or GPVI-CD39-coated nanoparticles and their impact on in vitro thrombus formation. *Int J Mol Sci* 2021;23(01):11
- 28 Puri RN, Colman RW. ADP-induced platelet activation. *Crit Rev Biochem Mol Biol* 1997;32(06):437–502
- 29 Gawaz M, Geisler T, Borst O. Current concepts and novel targets for antiplatelet therapy. *Nat Rev Cardiol* 2023;20(09):583–599
- 30 Daniel JL, Dangelmaier C, Jin J, Ashby B, Smith JB, Kunapuli SP. Molecular basis for ADP-induced platelet activation. I. Evidence for three distinct ADP receptors on human platelets. *J Biol Chem* 1998;273(04):2024–2029
- 31 Ollivier V, Syvannarath V, Gros A, et al. Collagen can selectively trigger a platelet secretory phenotype via glycoprotein VI. *PLoS One* 2014;9(08):e104712
- 32 Roberts DE, McNicol A, Bose R. Mechanism of collagen activation in human platelets. *J Biol Chem* 2004;279(19):19421–19430
- 33 Shibata M, Watanabe H, Uchihashi T, Ando T, Yasuda R. High-speed atomic force microscopy imaging of live mammalian cells. *Biophys Physicobiol* 2017;14:127–135
- 34 Rheinlaender J, Geisse NA, Proksch R, Schäffer TE. Comparison of scanning ion conductance microscopy with atomic force microscopy for cell imaging. *Langmuir* 2011;27(02):697–704
- 35 Novak P, Li C, Shevchuk AI, et al. Nanoscale live-cell imaging using hopping probe ion conductance microscopy. *Nat Methods* 2009;6(04):279–281
- 36 Lang F. Mechanisms and significance of cell volume regulation. *J Am Coll Nutr* 2007;26(5, Suppl):613S–623S
- 37 Rheinlaender J, Schäffer TE. Lateral resolution and image formation in scanning ion conductance microscopy. *Anal Chem* 2015;87(14):7117–7124
- 38 Nobel PS. The Boyle-Van't Hoff relation. *J Theor Biol* 1969;23(03):375–379
- 39 Zhou EH, Trepatt X, Park CY, et al. Universal behavior of the osmotically compressed cell and its analogy to the colloidal glass transition. *Proc Natl Acad Sci USA* 2009;106(26):10632–10637
- 40 Simeonov S, Schäffer TE. High-speed scanning ion conductance microscopy for sub-second topography imaging of live cells. *Nanoscale* 2019;11(17):8579–8587
- 41 Watanabe S, Kitazawa S, Sun L, Koder N, Ando T. Development of high-speed ion conductance microscopy. *Rev Sci Instrum* 2019;90(12):123704
- 42 Summerer MH, Genco PV, Katz AJ. The response of human platelets to hypotonic stress: direct measurement of volume change. *Ann Clin Lab Sci* 1978;8(06):447–452
- 43 Meyer MM, Verkman AS. Human platelet osmotic water and nonelectrolyte transport. *Am J Physiol* 1986;251(4, Pt 1):C549–C557
- 44 Wong KR, Verkman AS. Human platelet diffusional water permeability measured by nuclear magnetic resonance. *Am J Physiol* 1987;252(6, Pt 1):C618–C622
- 45 Watanabe E, Sasakawa S. Changes of platelet cell volumes in hypotonic solution. *Thromb Res* 1983;31(01):13–21
- 46 Wright JR, Mahaut-Smith MP. Why do platelets express K⁺ channels? *Platelets* 2021;32(07):872–879
- 47 Hoffmann EK, Dunham PB. Membrane mechanisms and intracellular signalling in cell volume regulation. *Int Rev Cytol* 1995;161:173–262

- 48 O'Neill WC. Physiological significance of volume-regulatory transporters. *Am J Physiol* 1999;276(05):C995–C1011
- 49 Beck F, Geiger J, Gambaryan S, et al. Temporal quantitative phosphoproteomics of ADP stimulation reveals novel central nodes in platelet activation and inhibition. *Blood* 2017;129(02):e1–e12
- 50 Trumel C, Payrastra B, Plantavid M, et al. A key role of adenosine diphosphate in the irreversible platelet aggregation induced by the PAR1-activating peptide through the late activation of phosphoinositide 3-kinase. *Blood* 1999;94(12):4156–4165
- 51 Margalit A, Livne AA. Lipoxygenase product controls the regulatory volume decrease of human platelets. *Platelets* 1991;2(04):207–214
- 52 von Kügelgen I, Hoffmann K. Pharmacology and structure of P2Y receptors. *Neuropharmacology* 2016;104:50–61
- 53 de Silva HA, Carver JG, Aronson JK. Pharmacological evidence of calcium-activated and voltage-gated potassium channels in human platelets. *Clin Sci (Lond)* 1997;93(03):249–255
- 54 Jennings LK, Fox JE, Edwards HH, Phillips DR. Changes in the cytoskeletal structure of human platelets following thrombin activation. *J Biol Chem* 1981;256(13):6927–6932
- 55 Roskopf D. Sodium-hydrogen exchange and platelet function. *J Thromb Thrombolysis* 1999;8(01):15–24
- 56 Díaz-Ricart M, Arderiu G, Estebanell E, et al. Inhibition of cytoskeletal assembly by cytochalasin B prevents signaling through tyrosine phosphorylation and secretion triggered by collagen but not by thrombin. *Am J Pathol* 2002;160(01):329–337
- 57 May JA, Glenn JR, Spangenberg P, Heptinstall S. The composition of the platelet cytoskeleton following activation by ADP: effects of various agents that modulate platelet function. *Platelets* 1996;7(03):159–168
- 58 Blase C, Becker D, Kappel S, Bereiter-Hahn J. Microfilament dynamics during HaCaT cell volume regulation. *Eur J Cell Biol* 2009;88(03):131–139
- 59 Galizia L, Pizzoni A, Fernandez J, Rivarola V, Capurro C, Ford P. Functional interaction between AQP2 and TRPV4 in renal cells. *J Cell Biochem* 2012;113(02):580–589
- 60 Casella JF, Flanagan MD, Lin S. Cytochalasin D inhibits actin polymerization and induces depolymerization of actin filaments formed during platelet shape change. *Nature* 1981;293(5830):302–305
- 61 Beussman KM, Mollica MY, Leonard A, et al. Black dots: High-yield traction force microscopy reveals structural factors contributing to platelet forces. *Acta Biomater* 2023;163:302–311
- 62 Paknikar AK, Eltzner B, Köster S. Direct characterization of cytoskeletal reorganization during blood platelet spreading. *Prog Biophys Mol Biol* 2019;144:166–176
- 63 Zaninetti C, Sachs L, Palankar R. Role of platelet cytoskeleton in platelet biomechanics: current and emerging methodologies and their potential relevance for the investigation of inherited platelet disorders. *Hamostaseologie* 2020;40(03):337–347
- 64 Downey GP, Grinstein S, Sue-A-Quan A, Czaban B, Chan CK. Volume regulation in leukocytes: requirement for an intact cytoskeleton. *J Cell Physiol* 1995;163(01):96–104
- 65 Peckys DB, Kleinhans FW, Mazur P. Rectification of the water permeability in COS-7 cells at 22, 10 and 0°C. *PLoS One* 2011;6(08):e23643
- 66 Armitage WJ, Juss BK. Osmotic response of mammalian cells: effects of permeating cryoprotectants on nonsolvent volume. *J Cell Physiol* 1996;168(03):532–538
- 67 Hagen I. Effects of thrombin on washed, human platelets: changes in the subcellular fractions. *Biochim Biophys Acta* 1975;392(02):242–254
- 68 Baenziger NL, Brodie GN, Majerus PW. Isolation and properties of a thrombin-sensitive protein of human platelets. *J Biol Chem* 1972;247(09):2723–2731
- 69 Siffert W, Siffert G, Scheid P, Akkerman JW. Activation of Na⁺/H⁺ exchange and Ca²⁺ mobilization start simultaneously in thrombin-stimulated platelets. Evidence that platelet shape change disturbs early rises of BCECF fluorescence which causes an underestimation of actual cytosolic alkalization. *Biochem J* 1989;258(02):521–527
- 70 Reed GL, Fitzgerald ML, Polgár J. Molecular mechanisms of platelet exocytosis: insights into the “secret” life of thrombocytes. *Blood* 2000;96(10):3334–3342
- 71 Fernandez JM, Neher E, Gomperts BD. Capacitance measurements reveal stepwise fusion events in degranulating mast cells. *Nature* 1984;312(5993):453–455
- 72 Hsu-Lin S, Berman CL, Furie BC, August D, Furie B. A platelet membrane protein expressed during platelet activation and secretion. Studies using a monoclonal antibody specific for thrombin-activated platelets. *J Biol Chem* 1984;259(14):9121–9126
- 73 Apodaca G. Modulation of membrane traffic by mechanical stimuli. *Am J Physiol Renal Physiol* 2002;282(02):F179–F190
- 74 Henson JH. Relationships between the actin cytoskeleton and cell volume regulation. *Microsc Res Tech* 1999;47(02):155–162
- 75 Schäffer TE. Nanomechanics of molecules and living cells with scanning ion conductance microscopy. *Anal Chem* 2013;85(15):6988–6994
- 76 Chen C-C, Zhou Y, Baker LA. Scanning ion conductance microscopy. *Annu Rev Anal Chem (Palo Alto, Calif)* 2012;5:207–228